

Distribution of Persistent Currents in a Multi-Arm Mesoscopic Ring: A Theoretical Study

Santanu K. Maiti,^{1,2,*} Srilekha Saha,¹ and S. N. Karmakar¹

¹Theoretical Condensed Matter Physics Division, Saha Institute of Nuclear Physics,
Sector-I, Block-AF, Bidhannagar, Kolkata-700 064, India

²Department of Physics, Narasinha Dutt College, 129 Belilious Road, Howrah-711 101, India

We propose an idea to investigate persistent current in individual arms of a multi-arm mesoscopic ring. Following a brief description of persistent current in a traditional mesoscopic ring pierced by an Aharonov-Bohm (AB) flux ϕ , we examine the behavior of persistent currents in separate arms of a three-arm mesoscopic ring where upper and lower sub-rings are subject to AB fluxes ϕ_1 and ϕ_2 , respectively. The present analysis may provide a basic framework to study magnetic response in individual branches of any complicated quantum network.

PACS numbers: 73.23.-b, 73.23.Ra.

I. INTRODUCTION

Generation of persistent current in a normal metal mesoscopic ring threaded by an Aharonov-Bohm flux ϕ has been proposed over a number of decades. The appearance of discrete energy levels as we scale down the ring size and large phase coherence length L_ϕ comparable to the system size L at much low temperature allow a non-decaying current upon the application of an external magnetic flux ϕ . Following the pioneering work of Büttiker, Imry and Landauer [1], various efforts have been made to explore the basic mechanisms of persistent current in mesoscopic rings and cylinders [2–14]. Later, the existence of non-decaying current in these systems has also been verified through some nice experiments [15–18]. The behavior of persistent current in a mesoscopic ring/cylinder can be studied theoretically by several ways as available in the literature [1–14]. *In all these available procedures the response of the entire system is achieved only, but no information about the individual branches of the system can be explored though the response in separate branches is highly significant to elucidate the actual mechanism of electron transport in a more transparent way.* This was the main motivation behind studying magnetic response in individual arms of a quantum network and to the best of our knowledge the present scheme has not been mentioned earlier in the literature.

In this presentation we propose an idea to investigate magnetic response in individual branches of a quantum network. With a brief description of persistent current in a single-channel mesoscopic ring (see Fig. 1), pierced by an AB flux ϕ , we discuss elaborately the behavior of persistent currents in individual arms of a three-arm mesoscopic ring (see Fig. 2) where upper and lower sub-rings are subject to AB fluxes ϕ_1 and ϕ_2 , respectively. Studying the natures of persistent currents in individual arms, variation of persistent current for the entire

system can be easily explained. In this three-arm ring system we address an unconventional feature of persistent current when impurities are introduced only in the middle arm, keeping the other two arms, viz, upper and lower, free from any impurity. It shows that the current amplitude of the system increases with the increase of impurity strength in the strong impurity regime, while it decreases in the weak impurity regime. This phenomenon is completely different from traditional disordered rings, where current amplitude always decreases with the increase of disorder strength. Recently, some anomalous features of electron dynamics have been reported in few special types of nano-scale materials, where the charge scattering takes place mainly from the surface regions and not from the inner core regions [19, 20].

In what follows, we present the results. In Section II, we describe two different geometric models and theoretical formulation for the calculation. Section III contains the numerical results. Finally, summary of our work will be available in Section IV.

II. MODEL AND THEORETICAL FORMULATION

A. A simple ring

Let us start by referring to Fig. 1, where a mesoscopic ring is subject to an AB flux ϕ (measured in unit of the elementary flux quantum $\phi_0 = ch/e$). A tight-binding (TB) formalism is given for the description of the ring. Within the non-interacting picture the TB Hamiltonian for a N -site ring in Wannier basis looks in the form,

$$H = \sum_i \epsilon_i c_i^\dagger c_i + \sum_i v \left(c_{i+1}^\dagger c_i e^{j\theta} + c_i^\dagger c_{i+1} e^{-j\theta} \right) \quad (1)$$

where, ϵ_i is the site energy and v gives the nearest-neighbor hopping integral. Due to the presence of AB flux ϕ , a phase factor $\theta = 2\pi\phi/N$ appears in the Hamiltonian. c_i^\dagger (c_i) is the creation (annihilation) operator.

*Electronic address: santanu.maiti@saha.ac.in

The energy E_k corresponding to k -th energy eigenstate $|\psi_k\rangle$ can be obtained from the expression,

$$E_k = \langle \psi_k | \mathbf{H} | \psi_k \rangle \quad (2)$$

where, $|\psi_k\rangle = \sum_p a_p |p\rangle$. Here $|p\rangle$'s are the Wannier states

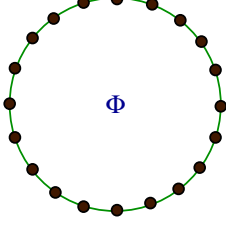


FIG. 1: (Color online). A mesoscopic ring threaded by an AB flux ϕ .

and a_p 's are the coefficients. Simplifying Eq. 2, we get the expression of the energy E_k as,

$$E_k = \sum_i \epsilon_i a_i^* a_i + \sum_i v [a_{i+1}^* a_i e^{j\theta} + a_i^* a_{i+1} e^{-j\theta}] \quad (3)$$

where, a_i^* is the complex conjugate of a_i . Here, the summation index i runs over all the atomic sites in the ring.

Now, the current carried by the k -th energy eigenstate $|\psi_k\rangle$ can be determined from the relation,

$$\begin{aligned} I_k &= -\frac{\partial E_k}{\partial \phi} \\ &= \frac{2\pi j v}{N} \sum_i [a_i^* a_{i+1} e^{-j\theta} - a_{i+1}^* a_i e^{j\theta}]. \end{aligned} \quad (4)$$

At absolute zero temperature ($T = 0\text{K}$), the net persistent current for a ring described with N_e electrons can be determined by taking the sum of individual contributions from the lowest N_e energy eigenstates. Therefore, for N_e electron system the net current becomes,

$$I = \sum_{k=1}^{N_e} I_k. \quad (5)$$

B. A three-arm ring

Following the above prescription, the distribution of persistent currents in individual arms, viz, upper, middle and lower, of a three-arm mesoscopic ring can be established. The schematic view of such a ring geometry is shown in Fig. 2, where a mesoscopic ring is partitioned symmetrically by a horizontal line to form two sub-rings, namely, upper and lower sub-rings and they are subject to AB fluxes ϕ_1 and ϕ_2 , respectively.

The TB Hamiltonian for this system is in the form,

$$\begin{aligned} \mathbf{H} &= \sum_i \epsilon_i c_i^\dagger c_i + \sum_i v_1 (c_{i+1}^\dagger c_i e^{j\theta_1} + c_i^\dagger c_{i+1} e^{-j\theta_1}) \\ &+ \sum_l \epsilon_l c_l^\dagger c_l + \sum_l v_2 (c_{l+1}^\dagger c_l e^{j\theta_2} + c_l^\dagger c_{l+1} e^{-j\theta_2}) \end{aligned} \quad (6)$$

where, the summation index i is used to refer the atomic sites in the upper and lower arms of the ring i.e., in the outer ring, while, the index l describes the atomic sites in the middle arm (filled black circles in the framed region). v_1 and v_2 describe the nearest-neighbor hopping integrals in the outer ring and middle arm, respectively. The phase

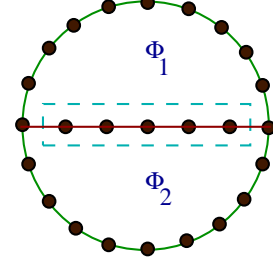


FIG. 2: (Color online). A three-arm mesoscopic ring, where the upper and lower sub-rings are subject to AB fluxes ϕ_1 and ϕ_2 , respectively.

factor θ_1 is associated with the hopping of an electron in the upper/lower arm, while in the middle arm it is described by the term θ_2 . They are represented as,

$$\theta_1 = \frac{\phi_1 + \phi_2}{N_U + N_L} \quad \text{and} \quad \theta_2 = \frac{\phi_1 - \phi_2}{2N_M} \quad (7)$$

where, N_U , N_M and N_L represent the total number of single bonds (a bond is formed by connecting two neighboring atoms through a line) in the upper, middle and lower arms of the ring, respectively. For this geometry E_k can be calculated according to the same prescription as given in Eq. 2 and with this energy expression we can determine the currents in individual arms. The expressions for the currents are as follows.

For the upper arm:

$$I_k^U = \frac{2\pi j v_1}{N_U + N_L} \sum_i [a_i^* a_{i+1} e^{-j\theta_1} - a_{i+1}^* a_i e^{j\theta_1}] \quad (8)$$

where, contributions from the N_U bonds are added.

For the middle arm:

$$I_k^M = \frac{\pi j v_2}{N_M} \sum_l [a_l^* a_{l+1} e^{-j\theta_2} - a_{l+1}^* a_l e^{j\theta_2}] \quad (9)$$

here, net contribution comes from N_M bonds.

For the lower arm:

$$I_k^L = \frac{2\pi j v_1}{N_U + N_L} \sum_i [a_i^* a_{i+1} e^{-j\theta_1} - a_{i+1}^* a_i e^{j\theta_1}] \quad (10)$$

here, the individual contributions of N_L bonds are added. Using these relations (Eq. 8-10), the net persistent currents at $T = 0\text{K}$ in individual arms of a three-arm mesoscopic ring containing N_e electrons can be obtained in the same fashion as mentioned in Eq. 5.

In the present work we perform all the characteristics of persistent current at $T = 0\text{K}$ and use the units where

$c = h = e = 1$. Throughout our numerical work we set all the nearest-neighbor hopping strengths (v , v_1 and v_2) to -1 and the energy scale is measured in unit of v .

III. NUMERICAL RESULTS AND DISCUSSION

A. A simple ring

As illustrative examples in Fig. 3 we show the current-flux characteristics for a single-channel impurity-free ($\epsilon_i = 0$ for all i) mesoscopic ring considering $N = 20$, where (a) and (b) correspond to the results for odd and even number of electrons, respectively. The red, green and blue curves in (a) represent the currents when $N_e = 3, 5$ and 9 , respectively, while in (b) these three

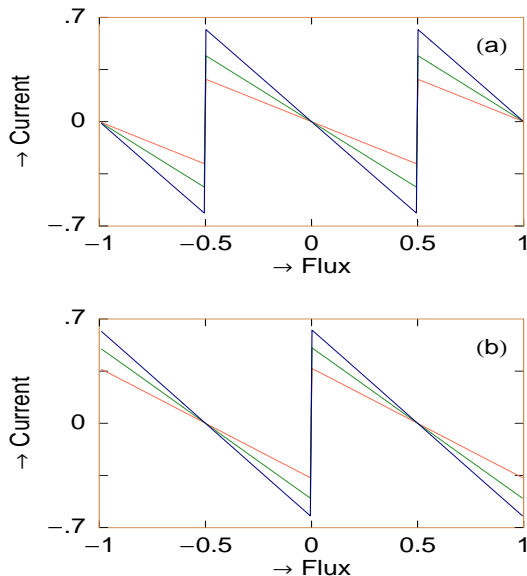


FIG. 3: (Color online). Current-flux characteristics of an ordered mesoscopic ring ($N = 20$) with (a) odd N_e and (b) even N_e . The red, green and blue curves in (a) correspond to $N_e = 3, 5$ and 9 , respectively, while in (b) these curves represent $N_e = 4, 6$ and 10 , respectively.

curves, respectively, represents the currents for $N_e = 4, 6$ and 10 . Both for the cases of odd and even N_e , current provides saw-tooth like nature with sharp jumps at half-integer or integer multiples of flux-quantum ϕ_0 depending on whether the ring is described by odd or even number of electrons. These currents are periodic in ϕ exhibiting ϕ_0 flux-quantum periodicity. The presented current-flux characteristics exactly match with the previous theoretical studies where persistent currents have been calculated by other approaches.

Thus, making sure with the results for a single-channel ring now we can safely use this procedure to illustrate the current-flux characteristics in individual arms of a three-arm mesoscopic ring.

B. A three-arm ring

1. Ring without any impurity

In Fig. 4 we present the variation of persistent current in individual arms of an ordered ($\epsilon_i = \epsilon_l = 0$ for all i and l) three-arm mesoscopic ring as a function of ϕ_1 , keeping the flux ϕ_2 constant. Here we consider $N_U = N_L = 10$, $N_M = 9$ and the flux ϕ_2 in the lower sub-ring is fixed at 0.3 . The individual currents in three different arms of the ring are evaluated for the total number of electrons $N_e = 10$, where (a), (b) and (c) correspond to the

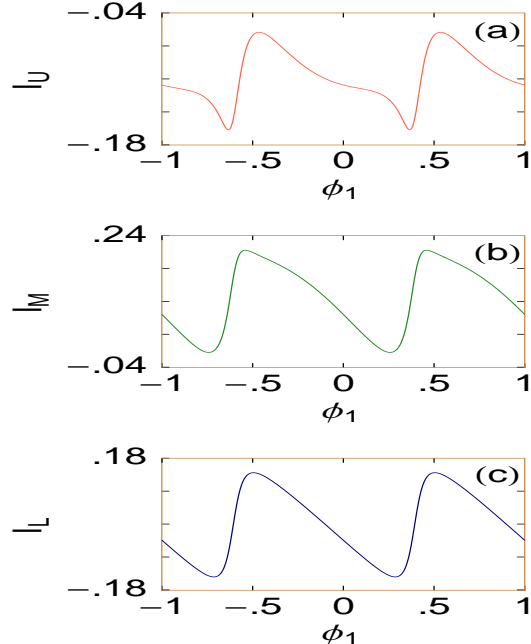


FIG. 4: (Color online). Persistent current in individual arms as a function of flux ϕ_1 for an ordered three-arm mesoscopic ring considering $N_U = N_L = 10$, $N_M = 9$, $\phi_2 = 0.3$ and $N_e = 10$, where (a), (b) and (c) correspond to the currents in the upper, middle and lower arms, respectively.

currents in the upper, middle and lower arms, respectively. These curves provide a complex spectra and it is noticed that the responses of the separate arms are quite different from each other. Most importantly we see that a significant change in amplitude takes place among the currents. By adding the currents (I_U , I_M and I_L) of the three different arms we get the net current of the entire mesoscopic ring and it becomes exactly identical to the current determined from the other conventional methods available in the literature. Thus, the net persistent current can be expressed through the relation $I_T = I_U + I_M + I_L$. Another important feature is that the sum of the currents carried by the upper and middle arms becomes exactly identical to the current carried by the lower arm i.e., we get another relation of current conservation as $I_L = I_U + I_M$. All these three currents

vary periodically with ϕ_1 showing ϕ_0 flux-quantum periodicity.

Now, instead of ϕ_1 if we display the variation of persistent current as a function of ϕ_2 , taking ϕ_1 as a constant, exactly similar features are observed as described above satisfying the current conservation relations.

2. Ring with impurities in the middle arm

Here we consider the diagonal disordered systems i.e., impurities are introduced only in the site energies without disturbing the hopping integral. To introduce impurities in the middle arm we choose the site energies of

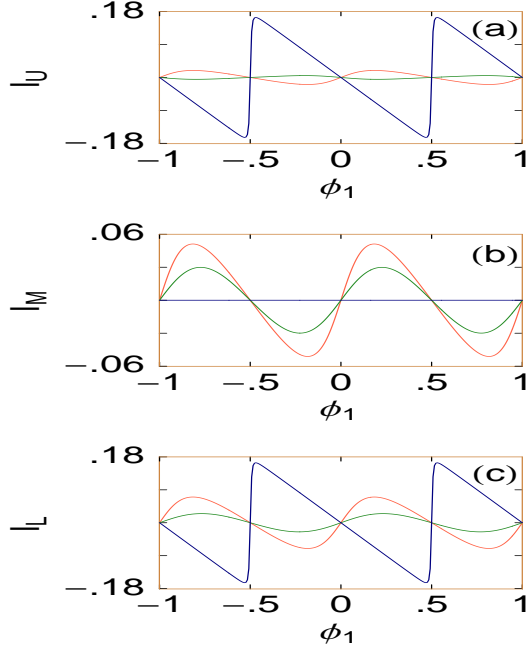


FIG. 5: (Color online). Current-flux characteristics for the three different arms of a three-arm mesoscopic ring considering $N_U = N_L = 15$, $N_M = 11$, $\phi_2 = 0.5$ and $N_e = 15$, where (a), (b) and (c) correspond to the currents in the upper, middle and lower arms, respectively. The red, green and blue curves in each panel represent $W = 0, 1$ and 10 , respectively.

the atomic sites, filled black circles in the framed region of Fig. 2, from a correlated distribution function which looks in the form,

$$\epsilon_l = W \cos(l\lambda\pi) \quad (11)$$

where, W is the strength of impurity. λ is an irrational number and we take $\lambda = (1 + \sqrt{5})/2$ for the sake of our illustration. Setting $\lambda = 0$, we get the perfect system with identical site energy W . Now, instead of considering site energies from a correlated distribution function (Eq. 11), we can also take them randomly from a “Box” distribution function of width W . In the later case we

have to take the average over a large number of disordered configurations and it takes much time to compute the results. Not only that, it does not provide any new result than the previous one where site energies are chosen from a correlated function.

As the middle arm is subject to impurities, while the others are free, we call this system as an ordered-disordered separated three-arm mesoscopic ring. In such a mesoscopic ring an unconventional feature of persistent current is observed when we tune the strength of

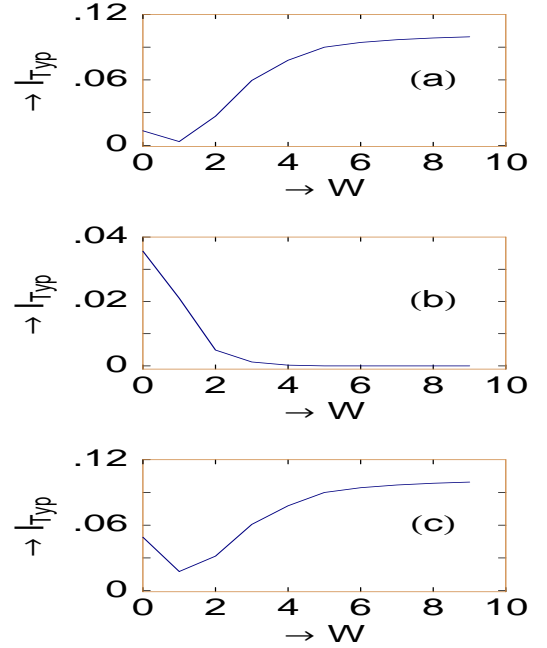


FIG. 6: (Color online). $I_{\text{typ}}-W$ characteristics of individual arms of a three-arm mesoscopic ring considering $N_U = N_L = 15$, $N_M = 11$, $\phi_2 = 0.5$ and $N_e = 15$, where (a), (b) and (c) correspond to the identical meaning as in Fig. 5.

disorder W . To emphasize it, in Fig. 5 we show the variation of persistent current in individual arms for a three-arm mesoscopic ring considering $N_U = N_L = 15$ and $N_M = 11$, where (a), (b) and (c) represent the currents in the upper, middle and lower arms, respectively. All these currents are determined at a fixed value of ϕ_2 ($\phi_2 = 0.5$) considering 15 electrons, where the red, green and blue lines in each panel correspond to $W = 0, 1$ and 10 , respectively. From the spectra it is observed that when $W = 1$ (weak), the current amplitude gets reduced (green curves) in all the three arms compared to the perfect case (red curves). The situation becomes completely different for the case of strong disorder i.e., $W = 10$. The current in the middle arm almost disappears (blue line in the middle panel), while for the other arms it achieves a high value (blue curves in the upper and lower panels). Thus a dramatic change in current amplitude takes place for the two different regimes of impurity strength. To explore this phenomenon more clearly, in Fig. 6, we show

the variation of typical current amplitude as a function of W , where (a), (b) and (c) give the results for the upper, middle and lower arms, respectively. The typical current amplitude is evaluated from the relation,

$$I_{\text{typ}} = \sqrt{\langle I^2 \rangle_{\phi_1}} \quad (12)$$

where, the averaging over a complete period of ϕ_1 is done. From the $I_{\text{typ}}-W$ spectra the effect of disorder is clearly

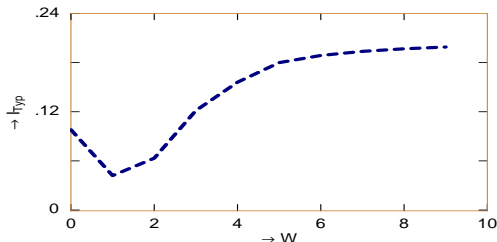


FIG. 7: (Color online). $I_{\text{typ}}-W$ spectrum for a three-arm mesoscopic ring with identical parameter values given in Fig. 6.

visible. It shows that the current amplitude in the middle arm sharply drops to zero as W is increased. While, for the other two impurity-free arms the current amplitude initially decreases, and reaching to a minimum at a critical value $W = W_c$ (say), it again increases with W . Thus, beyond the critical disorder strength W_c , the anomalous behavior is observed and this phenomenon can be implemented as follows. We consider the three-arm mesoscopic ring as a coupled system combining two sub-systems, one is ordered and other is disordered. In the absence of any coupling among the ordered and disordered regions, we can think the entire system as a simple combination of two independent sub-systems. Therefore, we get all the extended states in the ordered region, while the localized states are obtained in the disordered region. In this situation, the motion of an electron in any one region is not affected by the other. But for the coupled system, the motion of the electron is no more independent, and we have to take the combined effects coming from both the two regions. With the increase of disorder, the scattering effect becomes dominated more and thus the reduction of the current is expected. This scattering is due to the existence of the localized eigenstates in the disordered region. Now in the limit of weak disorder the coupling between the two sub-systems becomes strong and the motion of the electron in the ordered region is highly influenced by the disordered region. Therefore, the scattering effect

from both the two regions is quite significant and the current amplitude gets reduced. On the other hand, in the strong disorder regime the coupling between the two sub-systems becomes weak and the scattering effect from the ordered region is less significant, and it decreases with W . At the critical value W_c , we get a separation between the much weaker localized states and the strongly localized states. Beyond this value, the weaker localized states become more extended and the strongly localized states become more localized with the increase of W . In this situation, the current is obtained mainly from these nearly extended states which provide the larger current with W in the higher disorder regime.

Since the response of the entire system is obtained by adding the contributions from the separate branches, the nature of the net typical current amplitude of the ordered-disordered separated three-arm mesoscopic ring looks in the form as illustrated in Fig. 7. Here also the typical current amplitude shows identical variation with disorder like the upper and lower arms and this unconventional behavior of current amplitude is clearly justified from the above analysis.

IV. CONCLUDING REMARKS

To summarize, we have explored an idea to investigate the nature of persistent currents in individual branches of a multi-arm mesoscopic ring. Starting with a brief description of persistent current in a traditional single-channel mesoscopic ring, pierced by an AB flux ϕ , we have examined the characteristic features of persistent currents in separate arms of a three-arm mesoscopic ring where the upper and lower sub-rings are subject to AB fluxes ϕ_1 and ϕ_2 , respectively. Our analysis may provide a basic framework to address magnetic response in individual branches of any complicated quantum network.

In the present paper we have done all the calculations by ignoring the effects of temperature, electron-electron correlation, electron-phonon interaction, etc. We need further study by incorporating all these effects.

ACKNOWLEDGMENTS

We acknowledge with deep sense of gratitude the illuminating comments and suggestions we have received from Prof. S. Sil, Prof. B. Bhattacharyya, Moumita Dey and Paramita Dutta during the calculations.

-
- [1] M. Büttiker, Y. Imry, and R. Landauer, Phys. Lett. **96A**, 365 (1983).
 - [2] H. F. Cheung, Y. Gefen, E. K. Riedel, and W. H. Shih, Phys. Rev. B **37**, 6050 (1988).

- [3] H. F. Cheung and E. K. Riedel, Phys. Rev. Lett. **62**, 587 (1989).
- [4] G. Montambaux, H. Bouchiat, D. Sigeti, and R. Friesner, Phys. Rev. B **42**, 7647 (1990).

- [5] B. L. Altshuler, Y. Gefen, and Y. Imry, Phys. Rev. Lett. **66**, 88 (1991).
- [6] F. von Oppen and E. K. Riedel, Phys. Rev. Lett. **66**, 84 (1991).
- [7] A. Schmid, Phys. Rev. Lett. **66**, 80 (1991).
- [8] V. Ambegaokar and U. Eckern, Phys. Rev. Lett. **65**, 381 (1990).
- [9] G. Bouzerar, D. Poilblanc, and G. Montambaux, Phys. Rev. B **49**, 8258 (1994).
- [10] T. Giamarchi and B. S. Shastry, Phys. Rev. B **51**, 10915 (1995).
- [11] S. K. Maiti, Physica E **31**, 117 (2006).
- [12] S. K. Maiti, Int. J. Mod. Phys. B **21**, 179 (2007).
- [13] S. K. Maiti, Int. J. Mod. Phys. B **22**, 4951 (2008).
- [14] S. K. Maiti, Solid State Phenomena **155**, 87 (2009).
- [15] L. P. Levy, G. Dolan, J. Dunsmuir, and H. Bouchiat, Phys. Rev. Lett. **64**, 2074 (1990).
- [16] V. Chandrasekhar, R. A. Webb, M. J. Brady, M. B. Ketchen, W. J. Gallagher, and A. Kleinsasser, Phys. Rev. Lett. **67**, 3578 (1991).
- [17] E. M. Q. Jariwala, P. Mohanty, M. B. Ketchen, and R. A. Webb, Phys. Rev. Lett. **86**, 1594 (2001).
- [18] R. Deblock, R. Bel, B. Reulet, H. Bouchiat, and D. Mailly, Phys. Rev. Lett. **89**, 206803 (2002).
- [19] J. X. Zhong and G. M. Stocks, Nano. Lett. **6**, 128 (2006).
- [20] C. Y. Yang, J. W. Ding, and N. Xu, Physica B **394**, 69 (2007).